Heliyon 9 (2023) e20972

Contents lists available at ScienceDirect

Heliyon

journal homepage: www.cell.com/heliyon

Exploring pharmacokinetics of talazoparib in ABCB1/ABCG2-deficient mice using a novel UHPLC-MS/MS method

Zahra Talebi [a], Dominique A. Garrison [b], Eric D. Eisenmann [a], Kalindi Parmar [c], Geoffrey I. Shapiro [c,d], Michelle A. Rudek [b,e], Alex Sparreboom [a,**], Yan Jin [a,*]

[a] Division of Pharmaceutics and Pharmacology, College of Pharmacy, The Ohio State University, Columbus, OH, USA
[b] Division of Clinical Pharmacology, Department of Medicine, School of Medicine, Johns Hopkins University, Baltimore, MD, USA
[c] Center for DNA Damange and Repair, Dana-Farber Cancer Institute, Boston, MA, USA
[d] Department of Medical Oncology, Dana-Farber Cancer Institute, Boston, MA, USA
[e] The Sidney Kimmel Comprehensive Cancer Center at Johns Hopkins University, Baltimore, MD, USA

ARTICLE INFO

Keywords:
ABC transporters
Mouse plasma
Pharmacokinetics
Talazoparib
UHPLC-MS/MS

ABSTRACT

A rapid, sensitive, and simple UHPLC-MS/MS method for the determination of the PARP inhibitor talazoparib in mouse plasma was developed and validated using [^{13}C,$^{2}H_4$]-talazoparib as an internal standard (IS). The assay procedure involved extraction of talazoparib and the IS from plasma using a single-step deproteination and separation of the analytes was achieved on an ACQUITY UPLC RP18 HSS T3 column with a mobile phase gradient at a flow rate of 0.4 mL/min in a run time of 5 min. The calibration curve was linear ($r^2 > 0.99$) over the concentration range of 0.5–100 ng/mL, and 10-fold dilution of samples could be accurately quantitated. The matrix effect and mean extraction recovery for talazoparib were between 93.7-109% and 87.7–105%, respectively. Precision and percent bias of quality control samples were always less than ±15%, indicating reproducibility and accuracy of the method. Talazoparib demonstrated bench-top stability at room temperature for 6 h, auto-sampler and reinjection stability at 4 °C for at least 24 h, and no significant degradation was observed after three freeze-thaw cycles. The developed method was successfully applied to pharmacokinetic studies involving serial blood sampling after oral administration of talazoparib to wild-type mice and animals with a genetic deficiency of the efflux transporters ABCB1 (P-gp) and ABCG2 (BCRP). Together, our results demonstrate the successful development of a suitable analytical method for talazoparib in mouse plasma and suggest that mice are a useful model to evaluate transporter-mediated drug-drug interactions involving therapy with talazoparib.

1. Introduction

Talazoparib (BMN-673) is an FDA-approved poly (ADP-ribose) polymerase (PARP) inhibitor used in patients with deleterious germline BRCA-mutated, HER2-negative, locally advanced or metastatic breast cancer [1,2]. It exhibits more potent antitumor responses at lower concentrations than other PARP inhibitors [2,3]. The molecular mechanism of action of talazoparib involves selective

* Corresponding author
** Corresponding author
E-mail addresses: sparreboom.1@osu.edu (A. Sparreboom), jin.1134@osu.edu (Y. Jin).

https://doi.org/10.1016/j.heliyon.2023.e20972
Received 5 August 2023; Received in revised form 28 September 2023; Accepted 12 October 2023
Available online 13 October 2023

inhibition of PARP1/2 enzymes involved in the repair process of single-strand DNA breaks, as well as trapping of PARP1/2 at sites of DNA damage [4,5]. Clinical studies have demonstrated that talazoparib is orally bioavailable and has a relatively long terminal half-life (~50 h) that results in systemic accumulation with daily dosing, which in turn may contribute to clinically important hematological toxicities such as anemia and thrombocytopenia [6].

Talazoparib undergoes minimal metabolism and is primarily eliminated via renal excretion of unchanged drug [7]. Since talazoparib is a substrate of the ATP-binding cassette transporters ABCB1 (P-gp) and ABCG2 (BCRP) [8], which are highly expressed in intestinal enterocytes and mediate luminal efflux, close monitoring is recommended when talazoparib is co-administered with drugs that inhibit theses transporters [9]. This is because inhibition of these transport mechanisms by drugs co-administrated with talazoparib may result in increased systemic exposure to the PARP inhibitor and subsequently affect the risk of treatment-related toxicities [10] and/or progression-free survival in breast cancer patients [11]. However, details of the mechanisms that drive the absorption and disposition of talazoparib *in vivo* and the precise contribution of efflux transporters to the pharmacokinetic profile of talazoparib and its drug-drug interaction potential remain unclear.

In an attempt to address this knowledge deficit, and shed light on possible drug drug interactions with talazoparib, we set out to develop and validate an analytical method for the determination of talazoparib in mouse plasma using UHPLC-MS/MS and implemented the method in a pharmacokinetic study utilizing wild-type mice and animal lacking ABCB1 and ABCG2. Although there are some reports of successful implementations of HPLC-MS/MS methods designed to detect talazoparib in arious matrices they are mostly optimized for rat or human plasma and therefore require larger samples sizes which are not feasible in mouse studies [12–15]. The current study aims to address the best possible method to address this issue and provides insight into the mechanisms underlying drug-drug interaction liabilities with talazoparib that further contribute to the safe and effective use of this clinically important drug in patients with cancer.

2. Materials and methods

2.1. Chemical and reagents

Talazoparib sulfate (>99.9% purity) and the internal standard [^{13}C,$^{2}H_4$]-talazoparib (>98% purity; >99.0% ^{13}C, 98.0% ^{2}H) were purchased from Alsachim (Illkirch-Graffenstaden, France). Novobiocin sodium (>99.9% purity) was obtained from Selleck Chemicals (Houston, TX, USA), and LC-MS-grade formic acid (FA), methanol and acetonitrile were from Fisher Scientific (Fair Lawn, NJ, USA). Dimethylacetamide (purity ≥99.5%), dextrose (purity ≥99.5%), and phosphate-buffered saline, all essential components for formulating the drug dosage, were procured from Fisher Scientific (Fair Lawn, NJ, USA). Solutol® HS 15, with a free macrogol content ranging from 27.0% to 39.0% (g/100g), was sourced from Sigma-Aldrich (St. Louis, MO, USA) for the formulation preparation. Blank plasma samples were obtained from wild-type mice on an FVB strain (Taconic Biosciences, Cambridge City, IN, USA). Cardiac puncture was used to collect whole blood from mice into heparinized tubes, which subsequently underwent centrifugation at 13,000×*g* for 5 min to obtain plasma. The obtained plasma was promptly transferred onto dry ice and stored at −80 °C until measurement.

2.2. Chromatographic condition optimization

For analysis, a Vanquish UHPLC was coupled with a Quantiva triple quadrupole mass spectrometer obtained from Thermo Fisher Scientific (Waltham, MA, USA). The separation of analytes were done on an ACQUITY UPLC RP18 HSS T3 (2.1 mm × 100 mm, 1.8 μm; Waters, Milford, MA, USA) column in conjunction with an ACQUITY UPLC BEH C18 VanGuard Pre-column (2.1 mm × 5 mm, 1.7 μm; Waters). The column and the temperature-controlled autosampler were maintained at 40 °C and 4 °C, respectively. The mobile phase was designed as a compbination of solvent A (0.1% FA in water) and solvent B (0.1% FA in a 1:1 mixture of acetonitrile and methanol, v/v). A gradient elution was used for separation, lasting for 5.0 min and operating at a flow rate of 0.4 mL/min. The composition of solvent B remained at 20% during the first 0.5 min and was then gradually increased to 95% between 0.5 and 2.5 min. From 2.5 to 4.0 min, the composition of B was maintained at 95%, after which it rapidly transitioned to 20% at 4.01 min. Finally, the solvent B was held steady at 20% to reach equilibrium from 4.01 to 5.0 min. A volume of 3 μL of the extracted samples was injected for analysis.

The mass spectrometer designated parameters are as follows: 11.7 Arb for sheath gas, 8.9 Arb for aux gas, 1.6 Arb for sweep gas, 350 °C and 370 °C for ion transfer tube, and vaporizer temperature, respectively. A heated ESI was used to create the ion using with the ion spray voltage set at 3854.55 V in positive ion mode. The pressure of argon as the collision gas was set at 1.5 mTorr. Scheduled selective reaction monitoring (SRM) was employed for analysis of talazoparib and the internal standard. Detailed information is presented in Table 1. Data processing was done by utilizing Thermo Scientific Xcalibur (version 4.4.16.14, Thermo Fisher Scientific).

Table 1
LC-MS/MS conditions for talazoparib and the internal standard.

Analyte	Retention time (min)	Precursor (*m/z*)	Product (*m/z*)	Collision energy (V)	RF lens (V)
Talazoparib	2.69	381.22	298.13	30.15	96
[^{13}C,$^{2}H_4$]-talazoparib	2.69	386.20	303.08	29.85	116

2.3. Composition of working solution, calibration samples, and quality control

Two methanolic stock solutions of talazoparib and one methanolic stock solution of its internal standard were prepared at concentration of 1 and 5 mg/mL, respectively. Separate working solutions of talazoparib were prepared by diluting individual stock solutions with methanol, which were then used to freshly prepare the calibration standards and quality control (QC) samples on each day of analysis. The calibration curve consisted of seven non-zero calibrators at the following concentrations: 0.5, 2.5, 10, 25, 50, 75, and 100 ng/mL. QC samples were made at 5 different concentration levels, including the lower limit of quantification (LLOQ) at 0.5 ng/mL, low QC (LQC) at 1.5 ng/mL, medium QC (MQC) at 40 ng/mL, high QC (HQC) at 80 ng/mL, and above upper limit of quantification (AULQ) at 800 ng/mL, where AULQ was diluted by blank mouse plasma to 80 ng/mL (1:10 dilution, v/v) before sample preparation. An internal standard methanoic working solution (500 ng/mL) was prepared by diluting the stock solution of [^{13}C,$^{2}H_4$]-talazoparib. Solutions were kept at −20 °C and brought to room temperature prior to use.

2.4. Method validation

2.4.1. Specificity and selectivity

Specificity was tested by analyzing six different lots of plasma from untreated wild-type mice to ensure the absence of endogenous substances in the plasma that could potentially cause interference with talazoparib or its internal standard. To assess selectivity, chromatograms obtained from untreated mouse plasma were compared to those obtained from samples spiked with talazoparib. The peak area difference less than 20% indicate negligible effect from the endogenous substances.

2.4.2. Linearity, accuracy, and precision

A calibration curve was constructed from seven non-zero samples covering the range of concentrations from 0.5 to 100 ng/mL, including the LLOQ. Two calibration curves were analyzed per day by weighted ($1/x^2$) least-squares linear regression using the analyte to IS peak area ratios over four consecutive days. The calibration curve parameters were used to back-calculate concentrations and to obtain values for the QC samples and unknown samples by interpolation. Intra-day accuracy and precision were assessed by analyzing five replicates of the QC samples at each level in mouse plasma. Inter-day accuracy and precision were determined by analyzing five replicates of the described QC samples in section 2.3 over four consecutive days. The accuracy was evaluated by calculating the bias (%) between the mean experimental value and the nominal concentration, while intra- and inter-day precision were determined using the coefficient of variation (CV%) according to the following formula:

$$Accuracy\ (Bias\%) = [(Observed\ mean - Nominal)\ /\ Nominal)] \times 100\%$$

$$Intra-day\ Precision\ (CV\%) = (SD\ /\ Observed\ mean) \times 100\%$$

$$Inter-day\ Precision\ (CV\%) = (Average\ SD\ over\ 4\ days\ /\ Observed\ mean\ over\ 4\ days) \times 100\%$$

For accuracy, biases within 15% of their nominal values were considered acceptable, except at the LLOQ, where biases within 20% were permitted. In term of precision, both intra- and inter-day results at each QC level was required to be within 15%, with the exception of the LLOQ, which allowed the CV% up to 20%. In a similar way, deviations within 15% of their nominal values were considered acceptable for obtained interpolated concentrations in terms of precision and accuracy, except for the LLOQ (within 20%). All statistical analyses were preformed using a validated spreadsheet in Microsoft Excel.

2.4.3. Matrix effect and recovery

The matrix effect test was used to examine the presence of any component in biological samples that would influence the ionization of either talazoparib or the internal standard, using the proportion of spiked mobile phase solutions and unextracted samples. For evaluation of the extraction recoveries extracted sample mean response was divided by the unextracted (spiked blank plasma extract) sample mean at the same concentration and at the LQC, MQC and HQC samples. Three replicates of each QC level were prepared using the established extraction procedure. The mean matrix effect and extraction recovery are considered acceptable if CV% is less than 15% at tested QC levels.

2.4.4. Stability

Stability studies i.e. bench-top stability, autosampler stability, re-injection stability, and freeze-thaw stability were assessed at LQC and HQC levels and performed. For the bench-top stability assessment, QC samples were kept at ambient temperature for 6 h. Autosampler stability was evaluated by storing QC samples at 4 °C in the auto-sampler for 24 h before analysis. Re-injection stability was determined by reanalyzing the processed QC samples, which stored in the autosampler at 4 °C after 24 h from the first injection. Freeze-thaw stability was assessed by subjecting QC samples to a cycle of storage at −80 °C for 12 h followed by thawing at room temperature, and then freezing them again at −80 °C. The cycle was repeated three times to simulate typical conditions and evaluate the stability of the samples under such circumstances. The stability of talazoparib in different conditions was assumed if the measured concentrations were within 85%–115% of the corresponding nominal concentrations.

2.5. In vivo studies

2.5.1. Animal pharmacokinetic studies

The developed method was applied to an *in vivo* experiment examining the pharmacokinetics of orally-administered talazoparib in mice, using 4–5 animals per group. As previously described [16], pharmacokinetic studies were performed by administering talazoparib (0.5 mg/kg; p.o.) to adult female mice (12–20 weeks old) from an inbred wild-type FVB strain or mice lacking ABCB1A, ABCB1B, and ABCG2 on the same background strain [ABCB1/ABCG2(−/−) mice] (Taconic Biosciences, Cambridge City, IN, USA) [17]. The dose of 0.5 mg/kg talazoparib was based on previous research [18], and the drug was formulated in a mixture of dimethylacetamide (10%), Solutol HS (5%), and phosphate-buffered saline (85%). The final concentration of talazoparib in the oral dosing solution was 0.1 mg/mL. In select experiments, novobiocin (formulated in 5% Dextrose Injection, USP) or vehicle was administered by oral gavage 30 min before talazoparib at a dose of 50 mg/kg.

After administration of talazoparib, approximate 30-μL of each whole blood was collected from each mouse at specific time points: 5 min, 15 min, 30 min, 1 h, 2 h, and 4 h. During the time interval of 5–30 min, samples were collected using a sterile 5 mm Goldenrod animal lancet (Braintree Scientific, Braintree, MA, USA) from a submandibular vein and a heparinized capillary tube (Thermo Fisher Scientific). Samples collected at 1 h and 2 h were obtained from the retro-orbital venous plexus using capillary tubes after mice were anesthetized using 2% isoflurane. The final sample was collected by cardiac puncture. For all samples, plasma was obtained by collecting the supernatant from whole blood samples after centrifugation at 13,000×*g* immediately after collection. Plasma was

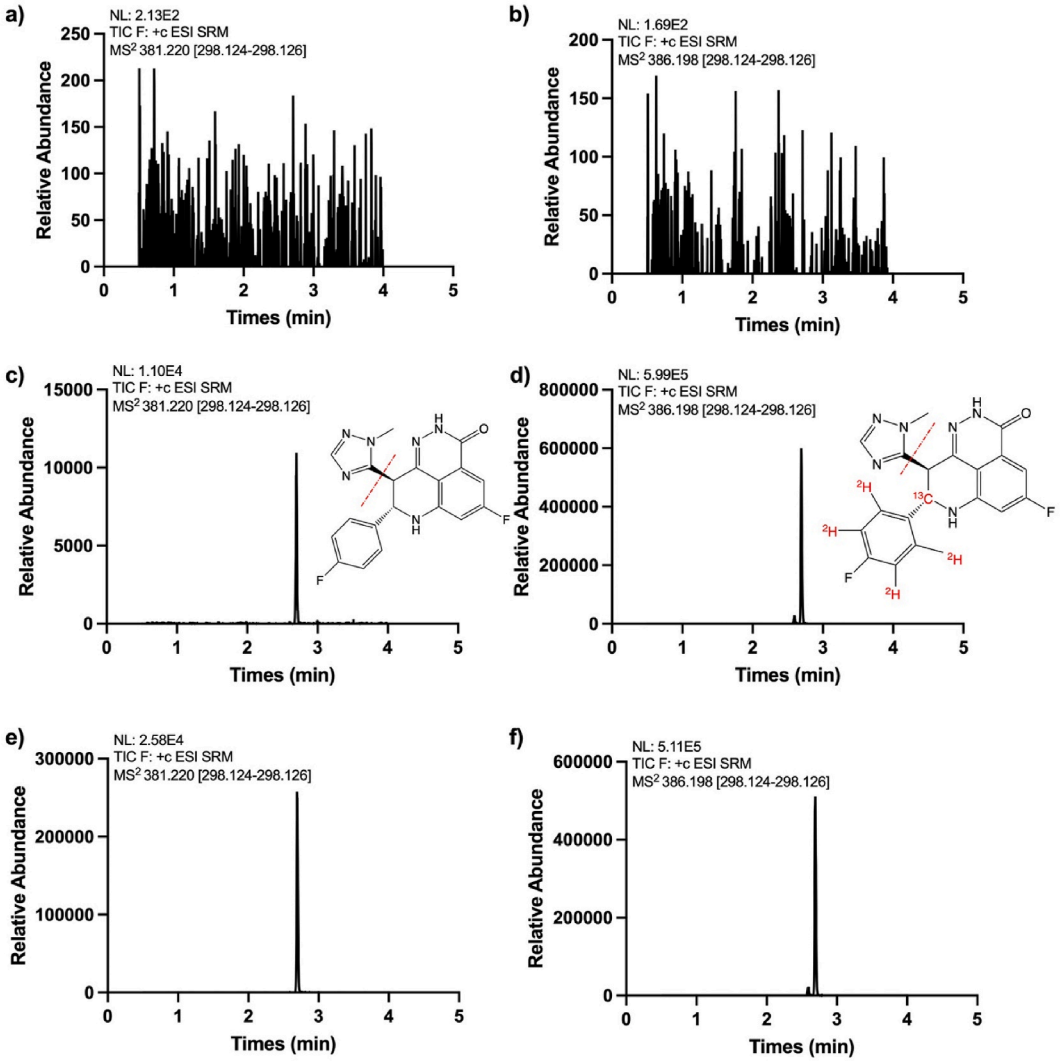

Fig. 1. Chromatograms of talazoparib and [^{13}C,^{2}H$_4$]-talazoparib in mouse plasma. Monitoring **(a)** talazoparib and **(b)** [^{13}C,^{2}H$_4$]-talazoparib in the blank plasma, **(c)** 0.5 ng/mL talazoparib spiked in the blank plasma with proposed fragmentation pathway, **(d)** 28.6 ng/mL [^{13}C,^{2}H$_4$]-talazoparib spiked in blank plasma with proposed fragmentation pathway, **(e)** talazoparib in plasma of a mouse, collected 5 min after oral administration of talazoparib (0.5 mg/kg), and (**f**) 28.6 ng/mL [^{13}C,^{2}H$_4$]-talazoparib added the sample in (e).

immediately placed on dry ice and stored at −80 °C until analysis. The pharmacokinetic experiments conducted at The Ohio State University was approved by the University Laboratory Animal Resources (ULAR) Animal Care and Use Committee. All used mice were housed with free access to water and a standard diet in a temperature- and light-controlled environment and were fasted for 2 h on the day of experiment before administration of talazoparib.

2.5.2. Sample preparation

Protein precipitation was performed with following procedure. Prior to analysis, 5-μL aliquots of plasma samples thawed at room temperature, were transferred into 0.5-mL Eppendorf tubes followed by 4 μL of 500 ng/mL internal standard working solution and 61 μL of methanol and then vortex-mixed for 30s The mixture in tubes were subjected to centrifugation at 15,000×*g* for 10 min at 4 °C. Subsequently, 55-μL of the resulting supernatant were carefully transferred to non-coated plastic microplates (96-well format, Thermo Fisher Scientific). A precise volume of 3 μL was injected into the LC-MS/MS system for analysis.

2.5.3. Analyzing pharmacokinetic data

Phoenix WinNonlin version 8.3.4.295 (Certara, Princeton, NJ, USA) was used to conduct non-compartmental analysis and derive pharmacokinetic parameters for talazoparib. Peak plasma concentration (C_{max}) was determined by visually examining the log concentration vs time curve. The area under the plasma concentration-time curve between time zero and the final collection point with detectable levels of talazoparib (AUC) was obtained using the log-linear trapezoidal rule. An unpaired Student's *t*-test was used to compare pharmacokinetic parameters of talazoparib between wild-type and ABCB1/ABCG2(−/−) mice or between treatments with and without novobiocin.

3. Results and discussion

3.1. Chromatographic and mass spectrometric conditions

A heated-ESI source operating in the positive ion mode was used to ionize talazoparib and its internal standard. Detection was performed in the SRM mode at *m/z* 381.22 → 298.13 for talazoparib and *m/z* 386.20 → 303.08 for [^{13}C,^{2}H$_4$]-talazoparib. Chromatographic conditions were optimized through several trials to achieve high resolution and symmetrical peak shapes, and with the final method, the observed average retention time for both talazoparib and the internal standard was 2.69 min (Fig. 1a–f).

3.2. Method validation

3.2.1. Specificity and selectivity

The specificity of the method was supported by the absence of endogenous interference(s) found around the retention time of talazoparib and its internal standard during analysis. Selectivity refers to the ability of the method to measure and differentiate the analyte despite the presence of endogenous and/or exogenous interferences, and the final optimized method provided adequate selectivity for the analysis of talazoparib in mouse plasma (Fig. 1a–f).

3.2.2. Linearity, accuracy, and precision

The calibration curves demonstrated acceptable linearity within the concertation range of 0.5–100 ng/mL. The mean (±SD) correlation coefficient (r^2) was determined to be 0.992 ± 0.0023 (range, 0.990–0.995) across four consecutive days during the employed validation strategy. As expected, good accuracy and precision was observed for talazoparib by using its stable-labeled analog [^{13}C,^{2}H$_4$]-talazoparib internal standards. Accuracy and precision results for talazoparib in QC samples are summarized in Table 2, and show that the intra-day precision, inter-day precision, and percent bias (accuracy) for LLOQ, LQC, MQC, and HQC samples ranged from 2.40% to 5.27%, 0.87%–2.00%, and -3.47%–8.35%, respectively. The intra-day precision, inter-day precision, and accuracy of AULQ samples after 10-fold dilution were 3.69%, 0.73%, and -1.44%, respectively. These finding suggest a high degree of reproducibility of the method and therefore the samples with concentrations higher than range in calibration curve can be further diluted and re-analyzed to get accurate results in the confirmed range of the calibration curve.

Table 2
Assay performance data for the quantitation of talazoparib in mouse plasma.

Sample	N	Nominal concentration (ng/mL)	Intra-day precision (CV%)	Inter-day precision (CV%)	Accuracy (bias%)
LLOQ	20	0.5	5.27	1.76	−1.52
LQC	20	1.5	5.27	1.33	−3.47
MQC	20	40	3.84	2.00	8.35
HQC	20	80	2.40	0.87	−3.25
AULQ (dilution 10x)	20	800	3.69	0.73	−1.44

Abbreviations: CV, coefficient of variation; LLOQ, The lower limit of quantification; LQC, low quality-control; MQC, medium quality-control, and HQC, high quality-control, AULQ, above upper limit of quantification.

3.2.3. Matrix effect and recovery

The matrix effect and extraction recovery results of QC samples at LQC, MQC, and HQC levels were well within the acceptable limit of ±15% (Table 3), indicating the lack of adverse matrix effects. An average recovery of >95% over the tested concentration ranges suggests the one-step protein-precipitation sample method is sufficient to extract talazoparib in plasma.

3.2.4. Stability

The stability studies conducted to simulate experimental conditions during actual sample analysis for the ongoing project indicate that talazoparib in mouse plasma samples remained stable for at least 6 h at room temperature (Table 4). Furthermore, the extracted talazoparib in methanol, prepared using the established extraction procedure, remained stable in the 4°C-temperature of the thermostatic auto-sampler for up to 24 h without any degradation. This indicates that re-injection of extracted samples can be done within 24 h without any loss in the assay performance. Results obtained after repeated freeze and thaw cycles demonstrated that talazoparib also remained stable in mouse plasma samples under the applied conditions, confirming that the integrity of the analyte was not affected by this process (Table 4).

3.3. Application to pharmacokinetic studies

The developed analytical method was next applied to measure plasma concentrations of talazoparib in mice after oral administration of the agent at a dose of 0.5 mg/kg (Fig. 2a). Although talazoparib is a transported substrate of ABCB1 and ABCG2 [8], efflux transporters in the intestine that restrict the absorption of several substrate drugs, deficiency of these transporters was not associated with any detectable changes in C_{max} and resulted in only a modest ~1.3-fold increase in AUC (Table 5). This observation is consistent with a previous report in which deficiency of both ABCB1 and ABCG2 in mice was associated with a similar increase in the observed plasma concentration of talazoparib 2 h after a single oral dose [19]. In that study, levels of talazoparib were found to be unaltered in plasma of mice with a deficiency of only ABCG2 and in MDCKII cells overexpressing ABCG2 [19], suggesting that talazoparib is unlikely to be sensitive to pharmacokinetic drug-drug interactions involving the concurrent use of ABCG2 inhibitors. This thesis is in line with our finding that pretreatment with novobiocin, a selective inhibitor of intestinal ABCG2 that does not affect ABCB1-mediated efflux [20], CYP3A4-mediated metabolism, or OATP1B1-mediated uptake [21], was not associated with substantially altered plasma levels of talazoparib in wild-type mice (Fig. 2b) or mice with a deficiency of both ABCB1 and ABCG2 (Fig. 2c; Table 6). These collective studies support the thesis that previously reported increases in exposure to talazoparib in humans receiving concurrent treatment with azole antifungal agents such itraconazole [9,22,23], which have a propensity to inhibit ABCB1 and ABCG2 with similar potency [24–26], can be attributed to modulation of ABCB1 activity.

4. Conclusion

We successfully developed and validated a simple, sensitive, robust, and reproducible UHPLC-MS/MS method for determining concentrations of the PARP inhibitor talazoparib in mouse plasma. Previous publications have reported LC-MS/MS assays that meet the sensitivity requirement for quantifying talazoparib in human liver microsomes [12], rat plasma [15], or human plasma [14] to support pharmacokinetics studies. However, these methods were developed in the context of studies in which relatively large volumes of biological fluid can be obtained (>50 μL), and thereby compromise application to the limited volumes that are available through repeat blood collection strategies in mice. Our method only requires plasma volumes of 5 μL that can be processed in a one-step deproteination, and the procedure is not dependent on drying steps employed in some earlier methods [19,27]. The quantification range we enable is between 0.5 and 100 ng/mL, allowing for accurate quantification of samples that are over-concentrated by a 10-fold dilution and all studies met their respective acceptability criteria. Application of the developed method to a murine pharmacokinetic study verified that the plasma levels of talazoparib are only modestly influenced by the simultaneous deficiency of the intestinal efflux transporters ABCB1 and ABCG2. In addition, our studies support the notion that pharmacokinetic drug-drug interactions between talazoparib and specific ABCG2 inhibitors such as novobiocin are highly unlikely given the limited contribution of this transporter to restrict movement of drug from the intestinal lumen to the systemic circulation. This finding may have clinical significance in that novobiocin has been shown to be an inhibitor of the helicase domain of the enzyme DNA polymerase theta (POLQ), and that combinatorial treatment regimens with novobiocin and talazoparib have shown promising activity in homologous-recombination deficient tumors, including those with acquired resistance against PARP inhibitors [28]. The developed method is presently being implemented in studies to further define the transporter-mediated mechanisms involved in the absorption and disposition of talazoparib in mice.

Table 3
Matrix effect and extraction recovery of talazoparib in mouse plasma.

		Matrix Effect		Recovery	
Concentration (ng/mL)	N	Mean Matrix Effect (%)	CV (%)	Mean Recovery (%)	CV (%)
1.5	3	109	5.6	87.7	14.4
40	3	95.6	5.24	105	4.91
80	3	93.7	13.1	92.7	0.88

Abbreviation: CV, coefficient of variation.

Table 4
Stability of talazoparib under various conditions.

Nominal (ng/mL)	N	Sample conditions							
		Bench-top[a]		Auto-sampler[b]		Re-injection[c]		Freeze-thaw[d]	
		Mean deviation (%)	CV (%)	Mean deviation (%)	CV (%)	Mean deviation (%)	CV (%)	Mean deviation (%)	CV (%)
1.5	3	2.15	13.5	−4.34	5.08	0.64	3.59	−3.18	1.99
80	3	−8.09	4.86	−5.14	7.22	0.62	1.66	−1.96	4.05

[a] The samples were subjected at ambient temperature (25 °C) for a duration of 6 h.
[b] Fresh samples were stored in the auto-sampler at 4 °C for 24 h.
[c] The analyzed samples were stored in the auto-sampler at 4 °C and reanalyzed samples after 24 h since the first injection.
[d] The samples underwent three freeze-thaw cycles.

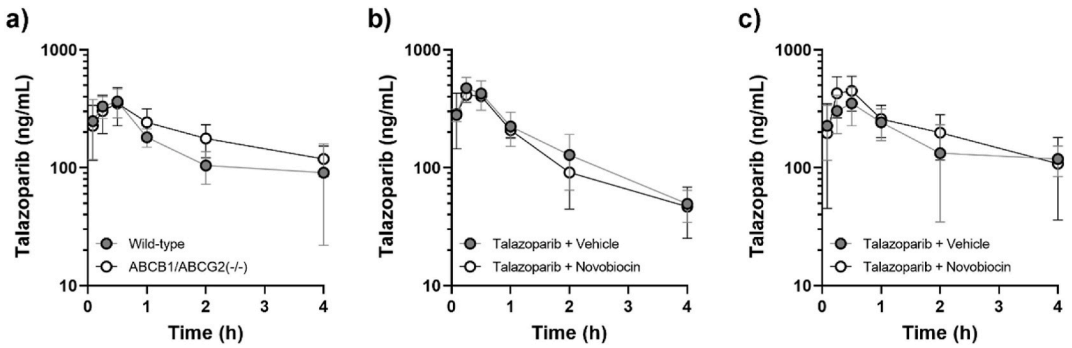

Fig. 2. Pharmacokinetic profile of talazoparib in wild-type mice and ABCB1/ABCG2(−/−) mice. (a) Plasma concentration-time curve of talazoparib in female wild-type FVB mice (n = 5) or ABCB1/ABCG2(−/−) mice (n = 4) after oral administration of a single dose of talazoparib (0.5 mg/kg). **(b)** Plasma concentration-time curve of talazoparib in female wild-type FVB mice (n = 5) after oral administration of a single dose of talazoparib (0.5 mg/kg), 30 min after a single oral dose of novobiocin (50 mg/kg) or vehicle. (**c**) Plasma concentration-time curve of talazoparib in female ABCB1/ABCG2(−/−) mice (n = 5) after oral administration of a single dose of talazoparib (0.5 mg/kg), 30 min after a single oral dose of novobiocin (50 mg/kg) or vehicle.

Table 5
Pharmacokinetic parameters of oral talazoparib in mice.[a]

Parameter	Wild-type mice	ABCB1/ABCG2(−/−) mice
C_{max} (ng/mL)	360 (±45)	350 (±63)
AUC (h × ng/mL)	620 (±80)	790 (±130)

Abbreviations: Cmax, peak plasma concentration; AUC, area under the plasma concentration-time curve between time zero and 4 h, the final collection time point with detectable drug levels.
[a] Data represent mean and ±SEM in parenthesis.N = 5 for Wild-type and N = 4 for ABCB1/ABCG2(−/−) mice.

Table 6
Influence of novobiocin on talazoparib pharmacokinetics in mice.[a]

Genotype	Co-treatment	C_{max} (ng/mL)	AUC (ng × h/mL)
Wild-type	None	472 (±56)	702 (±117)
Wild-type	Novobiocin	414 (±25)	615 (±41)
ABCB1/ABCG2(−/−)	None	352 (±63)	723 (±125)
ABCB1/ABCG2(−/−)	Novobiocin	449 (±74)	890 (±188)

Abbreviations: Cmax, peak plasma concentration; AUC, area under the plasma concentration-time curve between time zero and 4 h, the final collection time point with detectable drug levels.
[a] Data represent mean and ±SEM in parenthesis. N = 5 in each group.

Data availability statement

Data will be made available on request.

CRediT authorship contribution statement

Zahra Talebi: Data curation, Investigation, Methodology, Project administration, Validation, Visualization, Writing – original draft. **Dominique A. Garrison:** Investigation, Validation, Visualization, Writing – review & editing. **Eric D. Eisenmann:** Data curation, Formal analysis, Investigation, Software, Validation, Visualization, Writing – review & editing. **Kalindi Parmar:** Conceptualization, Funding acquisition, Resources, Writing – review & editing. **Geoffrey I. Shapiro:** Conceptualization, Funding acquisition, Resources, Writing – review & editing. **Michelle A. Rudek:** Conceptualization, Funding acquisition, Resources, Writing – review & editing. **Alex Sparreboom:** Conceptualization, Data curation, Funding acquisition, Methodology, Project administration, Resources, Supervision, Writing – review & editing. **Yan Jin:** Conceptualization, Data curation, Formal analysis, Investigation, Methodology, Project administration, Software, Validation, Visualization, Writing – original draft.

Declaration of competing interest

The authors declare that they have no known competing financial interests or personal relationships that could have appeared to influence the work reported in this paper.

Acknowledgments

This project was supported in part by the Experimental Therapeutics Clinical Trials Network (ETCTN) of the National Cancer Institute grant U24CA247648 (M A. Rudek, A. Sparreboom), the Clinical Pharmacology Training Program of the National Institutes of Health grant NIH T32GM066691 (D.A. Garrison), the OSU Comprehensive Cancer Center Pelotonia foundation (Z. Talebi, A. Sparreboom), and the Dana-Farber Cancer Institute discretionary funds supporting ETCTN activities under UM1CA186709 (G.I. Shapiro). The content of this publication is solely the responsibility of the authors and does not necessarily represent the official views of the funding agencies.

References

[1] J.K. Litton, et al., Talazoparib in patients with advanced breast cancer and a germline BRCA mutation, N. Engl. J. Med. 379 (8) (2018) 753–763.
[2] J. Murai, et al., Stereospecific PARP trapping by BMN 673 and comparison with olaparib and rucaparib, Mol. Cancer Ther. 13 (2) (2014) 433–443.
[3] Y. Shen, et al., BMN 673, a novel and highly potent PARP1/2 inhibitor for the treatment of human cancers with DNA repair deficiency, Clin. Cancer Res. 19 (18) (2013) 5003–5015.
[4] M. Rouleau, et al., PARP inhibition: PARP1 and beyond, Nat. Rev. Cancer 10 (4) (2010) 293–301.
[5] J. Murai, et al., Trapping of PARP1 and PARP2 by clinical PARP inhibitors, Cancer Res. 72 (21) (2012) 5588–5599.
[6] J. de Bono, et al., Phase I, dose-Escalation, two-Part Trial of the PARP inhibitor talazoparib in patients with advanced germline BRCA1/2 mutations and selected sporadic cancers, Cancer Discov. 7 (6) (2017) 620–629.
[7] Y. Yu, et al., A phase 1 mass balance study of (14) C-labeled talazoparib in patients with advanced solid tumors, J. Clin. Pharmacol. 59 (9) (2019) 1195–1203.
[8] G. Guney Eskiler, et al., Talazoparib nanoparticles for overcoming multidrug resistance in triple-negative breast cancer, J. Cell. Physiol. 235 (9) (2020) 6230–6245.
[9] Y. Yu, et al., Population pharmacokinetics of talazoparib in patients with advanced cancer, J. Clin. Pharmacol. 60 (2) (2020) 218–228.
[10] M. Elmeliegy, et al., Exposure-safety analyses of talazoparib in patients with advanced breast cancer and germline BRCA1/2 mutations in the EMBRACA and ABRAZO trials, J. Clin. Pharmacol. 60 (10) (2020) 1334–1343.
[11] Y. Yu, et al., Talazoparib exposure-efficacy analysis in patients with advanced breast cancer and germline BRCA1/2 mutations in the EMBRACA trial, J. Clin. Pharmacol. 60 (10) (2020) 1324–1333.
[12] M.W. Attwa, et al., Metabolic stability assessment of new PARP inhibitor talazoparib using validated LC-MS/MS methodology: in silico metabolic vulnerability and toxicity studies, Drug Des. Devel. Ther. 14 (2020) 783–793.
[13] S. Pakalapati, et al., Novel LC–MS method development and validation for characterization of talazoparib, an anti-cancer drug and its forced degradation behavior, Res. J. Pharm. Technol. 15 (6) (2022) 2592–2598.
[14] M.A.C. Bruin, et al., Development and validation of an integrated LC-MS/MS assay for therapeutic drug monitoring of five PARP-inhibitors, J. Chromatogr. B Analyt. Technol. Biomed. Life Sci. 1138 (2020), 121925.
[15] L. Ye, et al., UPLC-MS/MS method for the determination of talazoparib in rat plasma and its pharmacokinetic study, J. Pharm. Biomed. Anal. 177 (2020), 112850.
[16] A.F. Leblanc, et al., Murine pharmacokinetic studies, Bio-protocol 8 (20) (2018), e3056.
[17] J.W. Jonker, et al., Contribution of the ABC transporters Bcrp1 and Mdr1a/1b to the side population phenotype in mammary gland and bone marrow of mice, Stem Cell. 23 (8) (2005) 1059–1065.
[18] E.A.M. Ruigrok, et al., Preclinical assessment of the combination of PSMA-targeting radionuclide therapy with PARP inhibitors for prostate cancer treatment, Int. J. Mol. Sci. 23 (14) (2022).
[19] S.H. Kizilbash, et al., Restricted delivery of talazoparib across the blood-brain barrier limits the sensitizing effects of PARP inhibition on temozolomide therapy in glioblastoma, Mol. Cancer Ther. 16 (12) (2017) 2735–2746.
[20] Y. Su, et al., Using novobiocin as a specific inhibitor of breast cancer resistant protein to assess the role of transporter in the absorption and disposition of topotecan, J Pharm Pharm Sci 10 (4) (2007) 519–536.
[21] K. Suzuki, et al., Usefulness of novobiocin as a selective inhibitor of intestinal breast cancer resistance protein (Bcrp) in rats, Xenobiotica 50 (9) (2020) 1121–1127.
[22] M. Elmeliegy, et al., Evaluation of the effect of P-glycoprotein inhibition and induction on talazoparib disposition in patients with advanced solid tumours, Br. J. Clin. Pharmacol. 86 (4) (2020) 771–778.
[23] D. Zhao, X. Long, J. Wang, Transporter-mediated drug-drug interactions involving poly (ADP-ribose) polymerase inhibitors (Review), Oncol. Lett. 25 (4) (2023) 161.

[24] A. Gupta, J.D. Unadkat, Q. Mao, Interactions of azole antifungal agents with the human breast cancer resistance protein (BCRP), J Pharm Sci 96 (12) (2007) 3226–3235.
[25] V.J. Lempers, et al., Inhibitory potential of antifungal drugs on ATP-binding cassette transporters P-glycoprotein, MRP1 to MRP5, BCRP, and BSEP, Antimicrob. Agents Chemother. 60 (6) (2016) 3372–3379.
[26] L.M. Vermeer, et al., Evaluation of ketoconazole and its alternative clinical CYP3A4/5 inhibitors as inhibitors of drug transporters: the in vitro effects of ketoconazole, ritonavir, clarithromycin, and itraconazole on 13 clinically-relevant drug transporters, Drug Metab. Dispos. 44 (3) (2016) 453–459.
[27] D. Zhang, et al., A nano-liposome formulation of the PARP inhibitor Talazoparib enhances treatment efficacy and modulates immune cell populations in mammary tumors of BRCA-deficient mice, Theranostics 9 (21) (2019) 6224–6238.
[28] J. Zhou, et al., A first-in-class polymerase theta inhibitor selectively targets homologous-recombination-deficient tumors, Nat. Cancer 2 (6) (2021) 598–610.